Journal of Technical Physics, J. Tech. Phys., 31, 3—4, 355-372, 1990.
Polish Academy of Sciences, Institute of Fundamental Technological Research, Warszawa.

ROUTES TO CHAOS IN COMPLEX PHYSICAL SYSTEMS

J. AWREJCEWICZ (ŁÓDŹ)

1. Introduction

Investigations concerning simple nonlinear harmonically excited oscillators with one degree of freedom show different possibilities of transition from regular to chaotic motion [1, 2]. The transition can be analyzed by means of analytical or numerical methods [3 - 6]. Generally speaking, physical systems whose dynamics is governed by ordinary nonlinear differential equations cannot be fully investigated by means of analytical methods. Only in a very limited number of cases such equations have strict analytical solutions and therefore approximate analytical methods are used more often. Such methods, however, have a limited use, as they make it possible to analyse only weakly nonlinear systems. Moreover, they have a local character which makes it impossible to analyse the evolution of the investigated system with the change of a chosen parameter (or parameters). Additionally, the use of approximate analytical methods for systems with many degrees of freedom is very arduous—especially when evaluating their calculation accuracy.

The numerical methods have not such drawbacks and on their basis the scenarios leading from regular to chaotic motion will be observed in three different physical systems.

The first of the considered differential equation systems models the vibrations of human vocal cords and it is a system of "stiff" differential equations of the fifth order.

The second is a mechanical autonomous system with two degrees of freedom whose self-excited vibrations are generated by friction.

The third system considered is a nonautonomous mechanical one with two degrees of freedom.

The aim of this work is, on the one hand, to analyse the routes from regular to chaotic motion in complex physical systems and, on the other hand to show similarities to and differences from the routes to chaos observed in simple sinusoidally excited oscillators.

2. The Method of Analysis

The analysis of dynamics of the three systems will generally be the same. First, the equations governing the vibrations of the examined systems will be written. Then the equations will be rescaled and reduced to their dimensionless form. Thanks to this procedure the number of parameters in the equations will be reduced and, in addition, such equations can govern many other physical systems.

The next stage is the numerical analysis of the obtained dimensionless differential equations. Basically, two different numerical methods have been used to observe the

evolution of the examined system. Periodic orbits have been followed on the basis of the solution of the boundary value problem by means of the shooting method, while quasiperiodic and chaotic orbits have been observed by means of the methods based on the solution of initial value problem (time histories, attractor projections, frequency spectra, Poincaré maps or Lapunov exponents).

As the other type of methods is well known and widely used in observing chaotic motions, we shall reduce ourselves only to a short presentation of the first type of methods used here to analyse autonomous systems.

We take an approximate fixed point $x_F^{(k)}$ near the unknown "true" one and a numerical integration over the estimated period $T^{(k)}$ is carried out. Using the shooting method the transformation $\mathbf{M}(\mathbf{x}_F^{(k)}) = \mathbf{M}_F^{(k)}$, where k stands for the successive points of the transformation, is created. The error $\mathbf{E} = \mathbf{x}_F^{(k)} - \mathbf{M}_F^{(k)}$ shows the accuracy of the estimation (k). The Newton-Raphson procedure used here makes it possible to find the fixed transformation point we seek with a high degree of accuracy (then $\mathbf{E} \cong 0$).

The problem of the examination of stability is reduced to the analysis of linear differential equations with periodic coefficients

$$\Delta\mathbf{p}' = \mathbf{J}(\tau)\Delta\mathbf{p} = \left.\frac{\partial \mathbf{x}'}{\partial \mathbf{x}}\right|_{x_p(\tau)} \Delta\mathbf{p}, \tag{2.1}$$

where $\mathbf{J}(\tau+2\pi) = J(\tau)$ and $\Delta\mathbf{p}$ is the perturbation vector of the investigated periodic solution $\mathbf{y}_p(\tau)$.

The general solution of (2.1) is

$$\Delta\mathbf{p} = \boldsymbol{\varphi}(\tau)\Delta\mathbf{p}(0), \tag{2.2}$$

where $\boldsymbol{\varphi}(\tau) = \boldsymbol{\varphi}(\tau+2\pi)$ is the fundamental matrix.

The characteristic equation

$$\chi(\nu) = \det(\mathbf{H}_F - \nu\mathbf{1}) = 0, \tag{2.3}$$

where

$$\mathbf{H}_F = \boldsymbol{\varphi}(2\pi) = \frac{\partial \mathbf{G}_F}{\partial \mathbf{X}_F} \tag{2.4}$$

yields the characteristic multipliers. $\mathbf{H}_F$ is already known from the above mentioned iteration as the Jacobi matrix at the fixed point.

The characteristic multipliers are decisive for stability and bifurcation of the periodic orbit considered. In the case of simple eigenvalues of the matrix $\mathbf{H}_F$ three basic situations are possible [7]. If one of the characteristic multipliers is real and it traverses the unit circle of the complex plane with the parameter change in point -1 in the direction from the centre outwards, then from the considered periodic orbit branches a new one with the period two times greater as compared with the original one which at the same time loses stability. If one real characteristic multiplier traverses the unit circle of the complex plane with the parameter change in point $+1$ in the direction outwards from the centre, then from the considered periodic orbit a new periodic orbit can branch which has the period two times smaller than the original orbit or, as a result of the saddle-node bifuraction, a strange chaotic attractor can appear [1]. Last, if a pair of complex conjugate eigenvalues of H

traverses the elementary circle from the centre outwards, then a new periodic or quasi-periodic solution will appear. The direction of eigenvectors in the bifurcation point determines the direction of the new bifurcation solution.

3. Vibrations of Human Vocal Cords

CRONJAEGER [8] has presented the nonlinear mechanical model governing the dynamics of the vocal cords. A vocal cord has been modelled as a mass with two degrees of freedom. The stiffness and damping qualities of an anisotropic support of the mass correspond to the real properties of the vocal cord. In order to describe the possible contact of the vocal cords, the additional elastic element (a stiff nonlinear spring) has been included in the model. The stiffness of this element has been chosen so that for horizontal displacement of the mass approaching the origin (in the given coordinate system) the force in the spring increases to infinity. It is assumed that the air flow from the lungs is adiabatical and the Bernoulli suction effect is neglected. Lungs and the air passage have been modelled as a kettle with stiff walls. The real elastic properties of the lungs and the air passage have been additionaly included in the elastic properties of the air. The escaping air flow is proportional to the horizontal deflection of the vocal cords and the flow rate of the air—stream

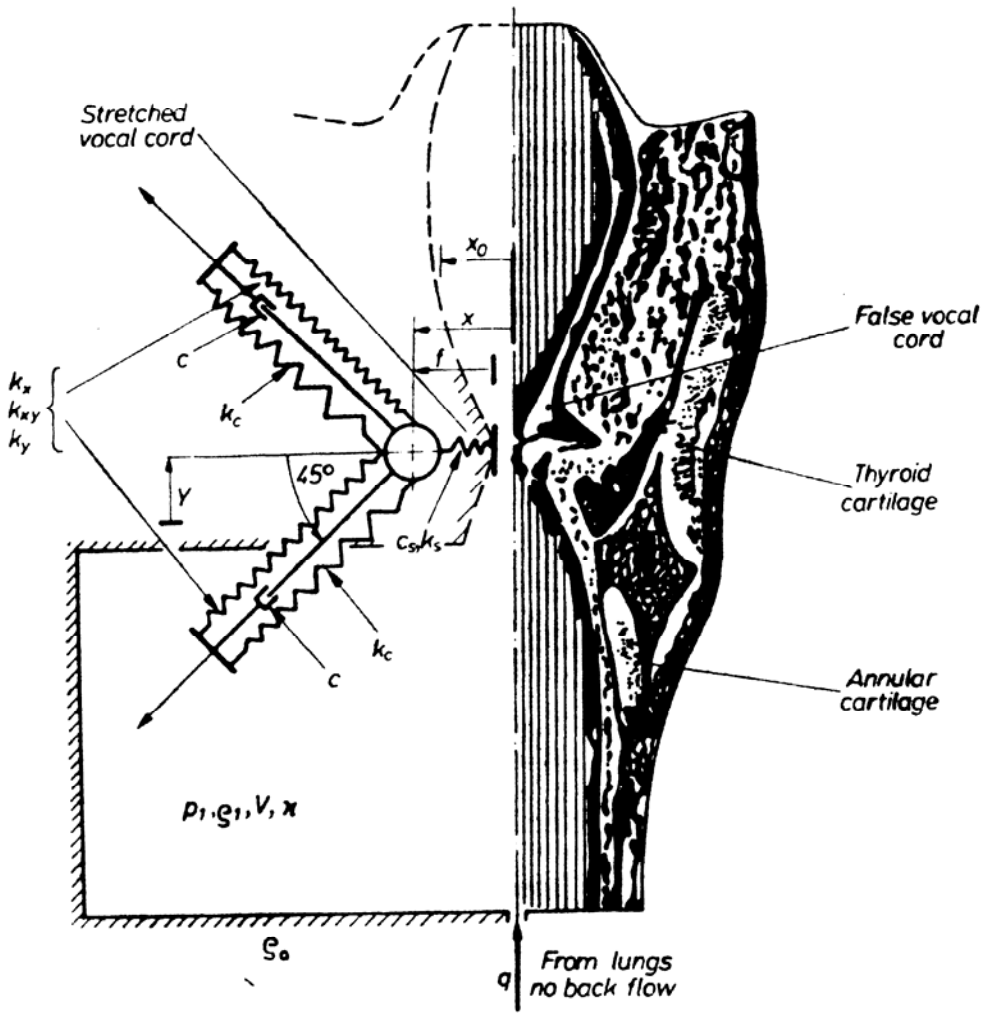

FIG. 1. Mechanical model of human vocal cords (on the basis of Cronjaeger's work [8]).

in the kettle. Pressure in the kettle creates approximately identical forces, both in the vertical and the horizontal directions of the displacement of the vocal cords.

The mechanical model of the human vocal cords is presented in Fig. 1. The coordinate system (x, y) describes horizontal and vertical displacements of the mass and p is subglottis pressure. The equilibrium point for the mass is $(x_0, 0)$, and f is a distance between the centre of the mass and the adge of the vocal cords. The air viscosity and inertia are neglected. The equations governing the dynamics of this system are:

$$
\begin{aligned}
&m\ddot{x}+c\dot{x}+\{k_x+k_c[x-x_0)^2+y^2)]\}(x-x_0)-k_{xy}y-k_s x^{-s}(1-c_s\dot{x}) = 0.5Ap,\\
&m\ddot{y}+c\dot{y}+\{k_y+k_c[(x-x_0)^2+y^2]\}y-k_{xy}(x-x_0) = 0.5Ap,\\
&\dot{p} = \frac{p_1 \varkappa}{\varrho_1 V}\begin{cases}\varrho_1 q-\dfrac{3}{4}\varrho_a h(x-f)(2\varrho_a^{-1}p)^{1/2} & \text{for} \quad x>f,\\ \varrho_1 q & \text{for} \quad x\leqslant f,\end{cases}
\end{aligned}
\tag{3.1}
$$

where m is the mass of the vocal cord $(0.24\cdot 10^{-3}$ kg); c is the damping of the vocal cord $(<4.10^{-4}$ Nsm$^{-1})$; k_x is the horizontal stiffness of the vocal cord $(k_x \in [20, 2000]$ Nm$^{-1})$; k_y is the vertical stiffness of the vocal cord $(k_y \in [0.7; 0.9]\, k_x)$; k_{xy} is the stiffness of the coupling between two directions of motion $(k_{xy} \in [0.3; 0.5]\, k_x)$; k_c is the Duffing's type stiffness $(<0.1\ k_x f^{-2})$; k_s is the additional stiffness of the vocal cords when brought together $(<0.1\, k_x f^{s+1})$; c_s is the additional damping of the vocal cords (when brought together); $s = 4$ (exponent); A is the vocal cord surface $(6.10^{-5}$ m$^2)$; ϱ_1 is the average subglottis air density (1.3 kgm^{-3}); ϱ_a is the average atmosphere density (1.25 kgm^{-3}); p_1 is the average subglottis pressure $(p_1 \in [1.01; 1.1]$ bar); f is the distance from the point-mass to the edge of the vocal cord $(3.10^{-3}$ m); q is the intensity of the air flow $(<6.10^{-4}$ m^{3}s$^{-1})$; V is the volume to the subglottis reservoir $(<3.10^{-3}$ m$^3)$; $\varkappa = 1.4$ (adiabatic exponent); h is the length of the vocal cord $(h \in [12; 18]\, 10^{-3}$ m).

In order to obtain the dimensionless equations, the following relations are taken:

$$
\begin{aligned}
\tau &= \omega t,\\
x(t) &= \alpha X(\tau),\\
y(t) &= \beta Y(\tau),\\
p(t) &= \mu P(\tau),\\
\alpha &= \beta = f,\\
\omega^2 &= k_x m^{-1},\\
\mu &= 2\left(\frac{3}{4}\frac{\varkappa}{\varrho_1}\frac{p_1 hf}{\omega V}\right)^2 \varrho a,
\end{aligned}
\tag{3.2}
$$

and the following dimensionless coefficients are introduced

$$
\begin{aligned}
C &= c(mk_x)^{-1/2},\\
K_y &= k_y k_x^{-1},\\
K_{xy} &= k_{xy} k_x^{-1},\\
K_c &= k_c f^2 k_x^{-1},
\end{aligned}
\tag{3.3}
$$

$$
\begin{aligned}
X_0 &= x_0 f^{-1}, \\
K_s &= k_s k_x^{-1} f^{-s-1}, \\
C_s &= f c_s (m k_x)^{-1/2}, \\
E &= 0.5 A (f k_x)^{-1} \mu, \\
Q &= \varkappa p_1 (V\mu)^{-1} q, \\
K_x &= k_x (m\omega^2)^{-1} = 1.
\end{aligned}
\tag{3.3 [cont.]}
$$

Introducing Eqs. (3.2) and (3.3) in (1.3), the following dimensionless system of equations is obtained:

$$
\begin{aligned}
&\ddot{X} + C\dot{X} + \{K_x + K_c[(X-X_0)^2 + Y^2]\}(X-X_0) - K_{xy} Y - K_s X^{-s}(1 - C_s \dot{X}) = EP, \\
&\ddot{Y} + C\dot{Y} + \{K_y + K_c[(X-X_0)^2 + Y^2]\} Y - K_{xy}(X-X_0) = EP, \\
&\dot{P} = Q - \begin{cases} (X-1)P^{1/2} & \text{for} \quad X > 1, \\ 0 & \text{for} \quad X \leqslant 1, \end{cases}
\end{aligned}
\tag{3.4}
$$

where $' = \dfrac{d}{d\tau}$.

The possible physical description of the new dimensionless coefficients with the intervals corresponding to the real properties of the vocal cords are given below.

C is the damping of the vocal cords (<1); K_y is the vertical stiffness of the vocal cords ($K_y \in [0.7; 0.9]$); $K_x = 1$; K_{xy} is the stiffness of the couplings between two directions of motion ($K_{xy} \in [0.1; 0.5]$); K_c is the Duffing's type stiffness (0.01); K_s is the hyperbolic type stiffness of the vocal cords when brought together (<0.01); $s = 4$; C_s is the damping of the vocal cords when brought together (<1); X_0 is the unloaded equilibrium position, position of the cartilage ($X_0 \in [0.1; 2.0]$); E is the average pressure or the vocal cord surface ($E \in [0.1; 10]$); Q is the intensity of the air stream ($Q \in [0; 100]$). The shooting and Newton–Raphson methods allow one to trace the fixed points of the Poincaré map (periodic orbits) with the change of parameters. In this case a linear prediction has been used. The eigenvalues of the numerically found Floquet matrix are the characteristic multipliers and affect the stability and bifurcation of the considered fixed points.

In order to normalize the period of the considered periodic orbit to 2π, a relative time $\tau_1 = \Omega\tau$ has been introduced during the numerical calculations. Frequency Ω enters the equations as a parameter to be obtained thanks to the freely chosen phase condition (in our case $\dot{X} = 0$). Because of the nonlinear term x^{-4}, standard methods based on the Runge–Kutta algorithm are not sufficiently accurate for integration of the system (3.4). A variable order, variable step Gear method has been used and calculations have been made with double precision.

In order to characterize the chaotic orbits the maximum one-dimensional Lapunov exponent λ_{max} has been calculated. This exponent has been determined by reducing (3.4) to a system of the first order differential equations

$$\dot{X} = X_1,$$
$$\dot{Y} = Y_1,$$

(3.5)

$$\dot{X}_1 = -CX_1 - \{K_x + K_c[(X-X_0)^2 + Y^2]\}(X-X_0) + K_{xy}Y + K_s X^{-s}(1 - C_s X_1) + EP,$$
$$\dot{Y}_1 = -CY_1 - \{K_y + K_c[(X-X_0)^2 + Y^2]\}Y + K_{xy}(X-X_0) + EP,$$
$$\dot{P} = Q - \begin{cases} (X-1)P^{1/2} & \text{for} \quad X > 1, \\ 0 & \text{for} \quad X \leqslant 1 \end{cases}$$

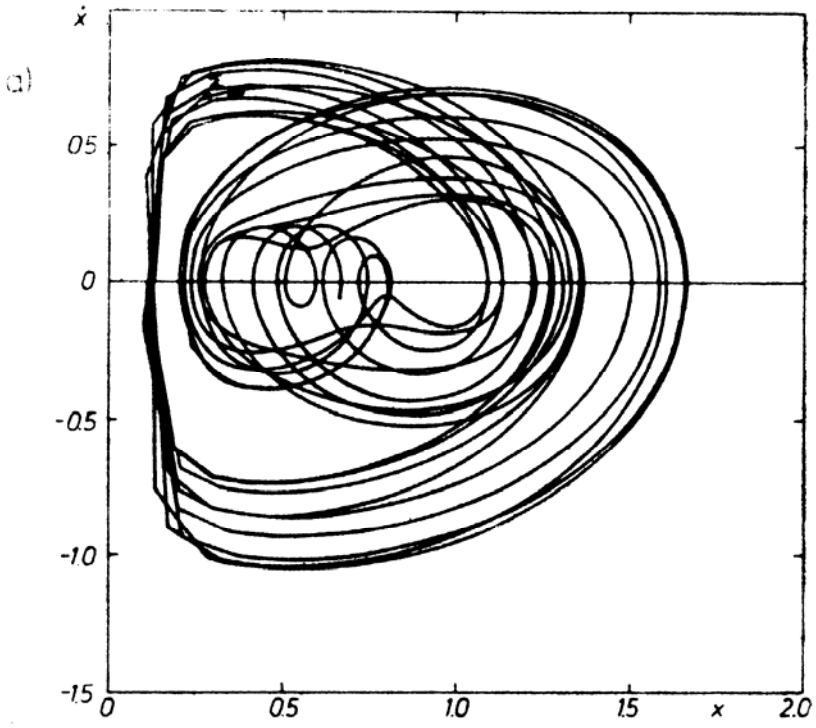

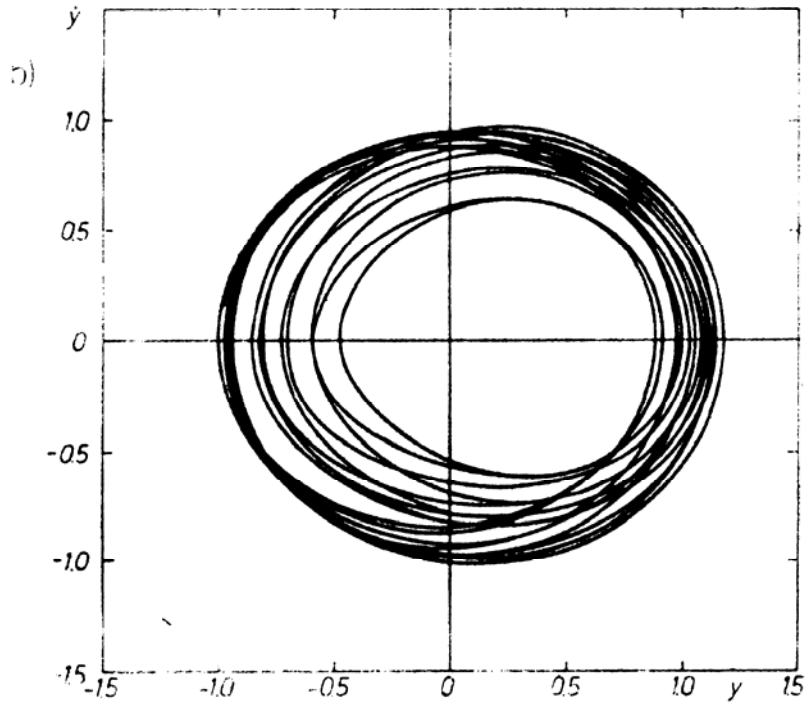

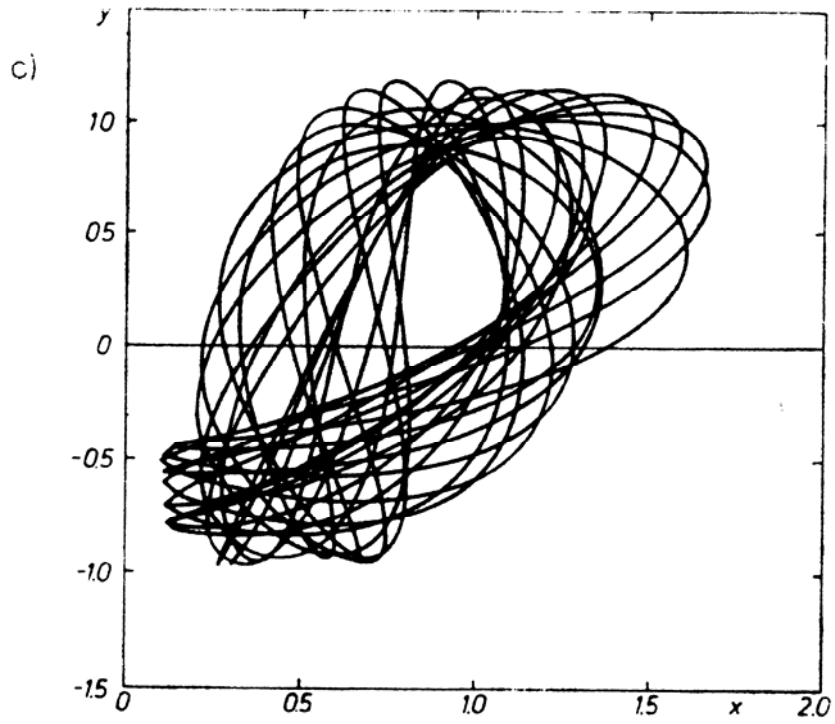

FIG. 2. Three projections of chaotic attractor in dynamic system (3.4).

and the system (3.5) together with its variational system has been solved numerically. A relatively large set of iterations is necessary to obtain the limit value (about 20,000 iterations have been used) for the considered differential equations.

The route to chaos has been examined for the following fixed parameters: $C = 0.001$, $K_x = 1.0$, $K_c = 0.001$, $X_0 = 0.6$, $K_{xy} = 0.3$, $K_s = 0.001$, $C_s = 0.5$, $E = 1.0$, $K_y = 0.9$. Q has been assumed as the bifurcation parameter. For $Q = 0.04$ a stable periodic orbit has been found which corresponds to the fixed point $X_0 = 1.5412$, $X_0' = 0$, $Y_0 = 1.0813$, $Y_0' = -2.1937$; $P_0 = 0.0184$; $\Omega = 0.9178$. In this case the characteristic multipliers have the values $\nu_{1,2} = -0.54 \pm i0.76$; $\nu_3 = 0.74$; $\nu_4 = 0.01$. The decrease of the bifurcation parameter leads to the loss of stability of the orbit. For example, for $Q = 0.02$ the characteristic multipliers are $\nu_{1,2} = -0.73 \pm 0.74i$, which means that for this value of Q the analysed periodic orbit is already unstable. In the moment when the value $(\mathrm{Re}(\nu_{1,2}) + \mathrm{Im}(\nu_{1,2})) = 1$ is exceeded, a quasiperiodic orbit appears. This orbit has been further observed on the basis of calculations of the maximum Lapunov exponent. It has been found out that the quasiperiodic orbit is very sensitive to the value Q changes. For $Q = 0.01$ the maximum Lapunov exponent is already positive and has the value 0.0128, which testifies to the occurrence of a chaotic orbit. Some of its projections are shown in Fig. 2.

4. Self-Excited Vibrations in a Mechanical System with Friction

The analysed system is presented in Fig. 3. The vibrations are due to the dependence of friction on the relative velocity, which for some velocity ranges has a falling character. When preparing the equations of motion, two possible states of the system were considered. When the disc moves in relation to the tape then the state is called the slip state, while

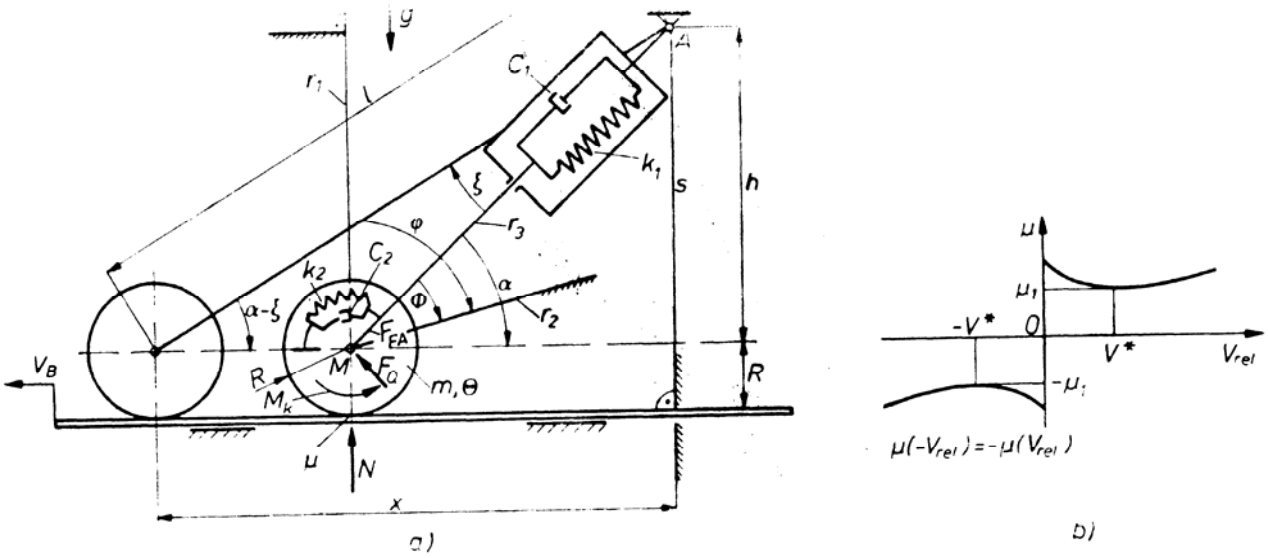

FIG. 3. Mechanical system with two degrees of freedom with given geometry and parameters which make it possible to derive equations of motion (a) and the dependence of friction coefficient on relative velocity (b)

when the disc does not move in relation to the tape we have the stick state. Other examples of transition to chaos in the system shown are presented in [9].

The relative velocity between the disc and the tape is

$$v_{rel} = v_B - \dot{\phi} R - \left(1 + \frac{Rh}{x^2+h^2}\right)\dot{x}. \tag{4.1}$$

The following equations of motion in the slip state are obtained

$$\mathbf{M}\begin{pmatrix}\ddot{x}\\ \ddot{\phi}\end{pmatrix} + \mathbf{B}\begin{pmatrix}\dot{x}\\ \dot{\phi}\end{pmatrix} + \mathbf{K}\begin{pmatrix}x\\ \phi\end{pmatrix} = \mu N\begin{pmatrix}1\\ R\end{pmatrix}, \tag{4.2}$$

where

$$\mathbf{M} = \begin{bmatrix} m & 0 \\ \Theta\dfrac{h}{l^2} & \Theta \end{bmatrix},$$

$$\mathbf{B} = \begin{bmatrix} \dfrac{x^2}{l^2}c_1 & -\dfrac{h}{l^2}c_2 \\ -2\Theta\dfrac{hx\dot{x}}{l^4} & c_2 \end{bmatrix}, \tag{4.3}$$

$$\mathbf{K} = \begin{bmatrix} \left(1-\dfrac{l_0}{l}\right)K_1 & -\dfrac{h}{l^2}K_2 \\ 0 & K_2 \end{bmatrix},$$

$$N = mg - \left\{\left(1-\frac{l_0}{l}\right)K_1 + \frac{\dot{l}}{l}c_1 + \frac{K_2}{l^2}\phi + \frac{c_2}{l^2}\dot{\phi}\right\}h,$$

$$(4.3)_{[\text{cont.}]}\quad \mu = \begin{cases} \operatorname{sign}(v_{\text{rel}})\left(\mu_1+\mu_2\left(1-\left|\dfrac{v_{\text{rel}}}{v^*}\right|\right)^2\right), & v_{\text{rel}} \neq 0, \\ \operatorname{sign}\left(\dfrac{d^i v_{\text{rel}}}{dt^i}\right)(\mu_1+\mu_2), & \dfrac{d^k v_{\text{rel}}}{dt^k} = 0 \quad \text{for} \quad k = 0 \ldots (i-1) \quad \text{and} \quad v_{\text{rel}} \neq 0, \\ \text{not defined for } v_{\text{rel}} \equiv 0. \end{cases}$$

In the stick state we have

$$(4.4)\qquad \left(\frac{\Theta}{R^2}+m\right)\ddot{x}+\left(1-\left(\frac{h}{l}\right)^2\right)c_1\dot{x}+\left(1-\frac{l_0}{l}\right)K_1 x = \left(\frac{1}{R}+\frac{h}{l^2}\right)(c_2\dot{\phi}+K_2\phi),$$

where

$$(4.5)\qquad \begin{aligned} \dot{\phi} &= \frac{v_B}{R}-\left\{\frac{1}{R}+\frac{h}{x^2+h^2}\right\}\dot{x}, \\ \phi &= \phi_H+\frac{v_B}{R}(t-t_H)-\frac{x-x_H}{R}-\arctan\left(\frac{x}{h}\right)+\arctan\left(\frac{x_H}{h}\right), \end{aligned}$$

and with H we mark the initial values of t, x, ϕ for the beginning of the stick.

By the use of transformations

$$(4.6)\qquad y_1 := \frac{x}{l_0}, \quad y_2 := y_1', \quad y_3 := \vartheta\phi, \quad y_4 := y_3', \qquad \tau := \sqrt{\frac{K_1}{m}}\,t \quad \text{and} \quad \frac{d(\,)}{d\tau} =: (\,)'$$

equations (4.2) with thirteen parameters l_0, h, R, K_1, m, Θ, g, c_1, c_2, v^*, v_B, μ_1, μ_2 are reduced to the dimensionless differential equations with eleven parameters χ, ϱ, $\varkappa$, γ, β_1, β_2, ϑ, V^*, V_B, μ_1, μ_2 of the following (first order) form at the slip-state:

$$(4.7)\qquad \begin{aligned} y_1' &= y_2, \\ y_2' &= -\left[\left(1-\frac{1}{\lambda}\right)+\frac{y_1 y_2}{\lambda^2}\beta_1\right](y_1+\mu\chi)-\frac{1}{\vartheta\varrho^2}(\beta_2 y_4+\varkappa y_3)\left(\frac{\mu y_1-\chi}{\lambda^2}\right)+\mu\gamma, \\ y_3' &= y_4, \\ y_4' &= -\vartheta\frac{\chi}{\lambda^2}\left(y_2'-2\frac{y_2^2 y_1}{\lambda^2}\right)-\frac{1}{\vartheta}\left(1+\frac{\mu}{\varrho}\frac{y_1}{\lambda^2}\right)(\beta^2 y_4+\varkappa y_3)- \\ &\qquad -\mu\varrho\left[\left(1-\frac{1}{\lambda}\right)\chi+\frac{y_1 y_2}{\lambda^2}\beta_1\chi-\gamma, \end{aligned}$$

where

$$(4.8)\qquad \lambda := l/l_0, \qquad \chi := \frac{h}{l_0}, \quad \varrho := \frac{l_0}{R}, \quad \varkappa := \frac{1}{R^2}\frac{K_2}{K_1}, \quad \gamma := \frac{mg}{K_1 l_0}, \quad \vartheta := \frac{\Theta}{mR^2},$$

$$B_1 := \frac{c_1}{\sqrt{K_1 m}}, \quad \beta_2 := \frac{1}{R^2}\frac{c_2}{\sqrt{K_1 m}}, \quad V^* := \frac{v^*}{l_0\sqrt{\frac{K_1}{m}}}, \quad V_B := \frac{v_B}{l_0\sqrt{\frac{K_1}{m}}}.$$

[364]

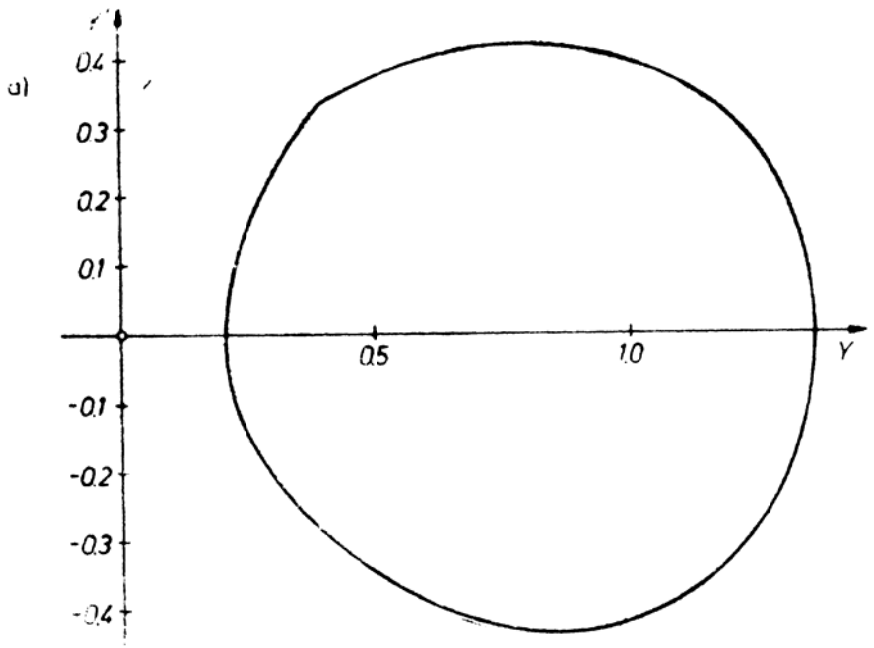
a)
0.4
0.3
0.2
0.1
-0.1
-0.2
-0.3
-0.4
0.5
1.0
Y

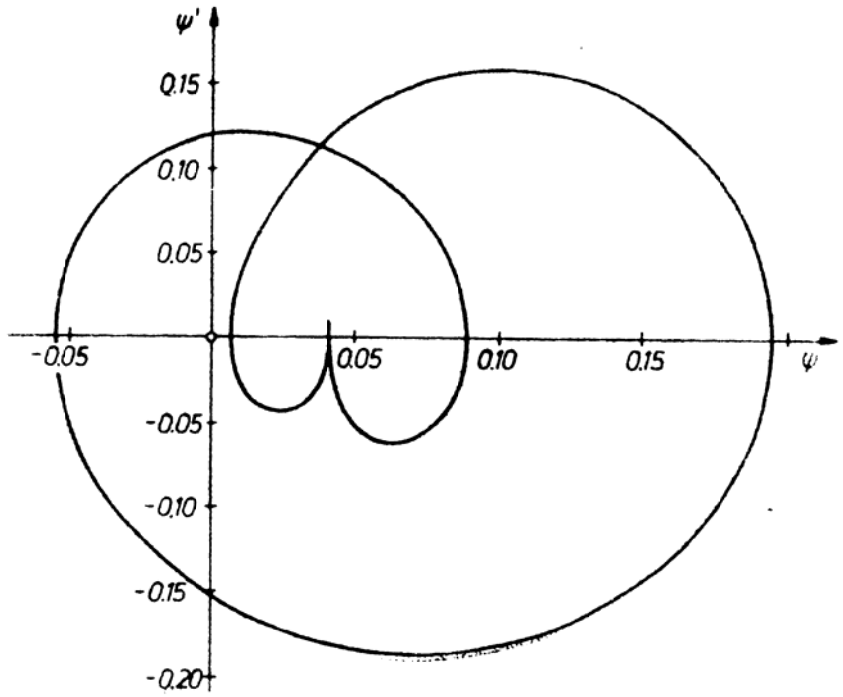
a)
ψ'
0.15
0.10
0.05
-0.05
-0.10
-0.15
-0.20
-0.05
0.05
0.10
0.15
ψ

[Fig. 4a]

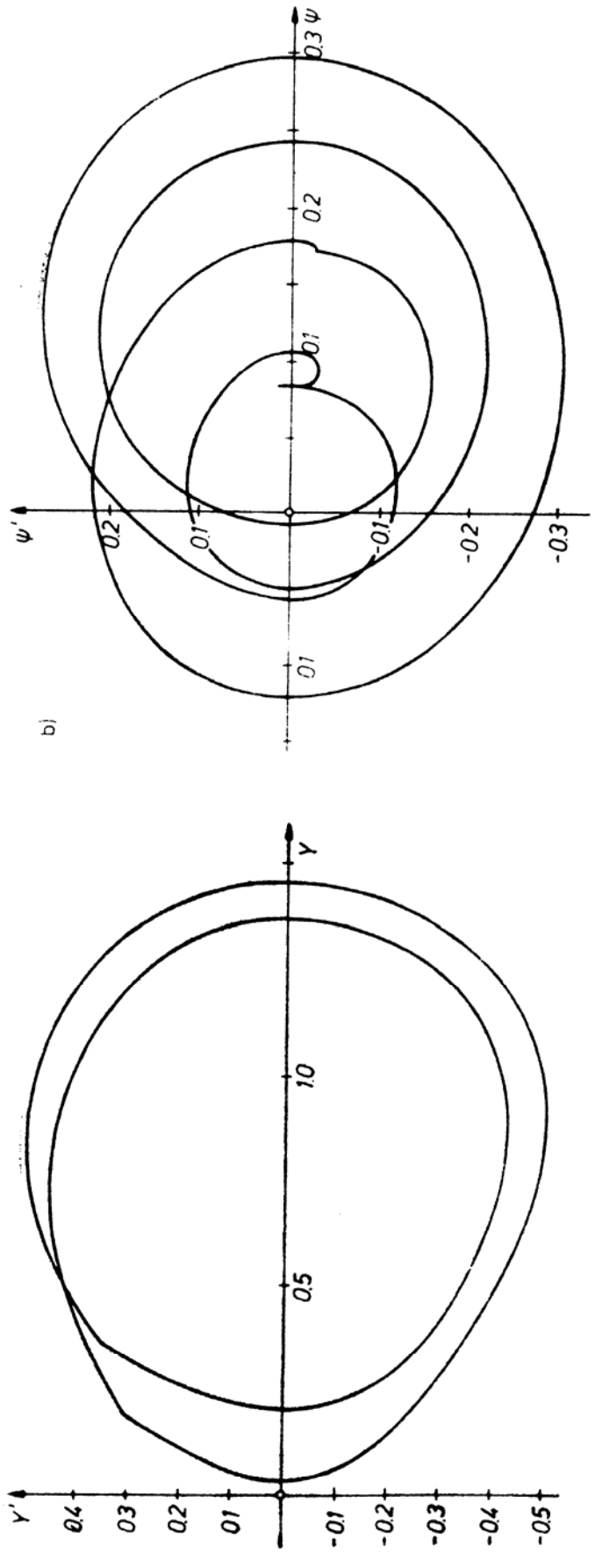

FIG. 4. Two projections of T-periodic (a) for $\gamma = 0.5$ and $2T$-periodic (b) for $\gamma = 0.65$ orbit.

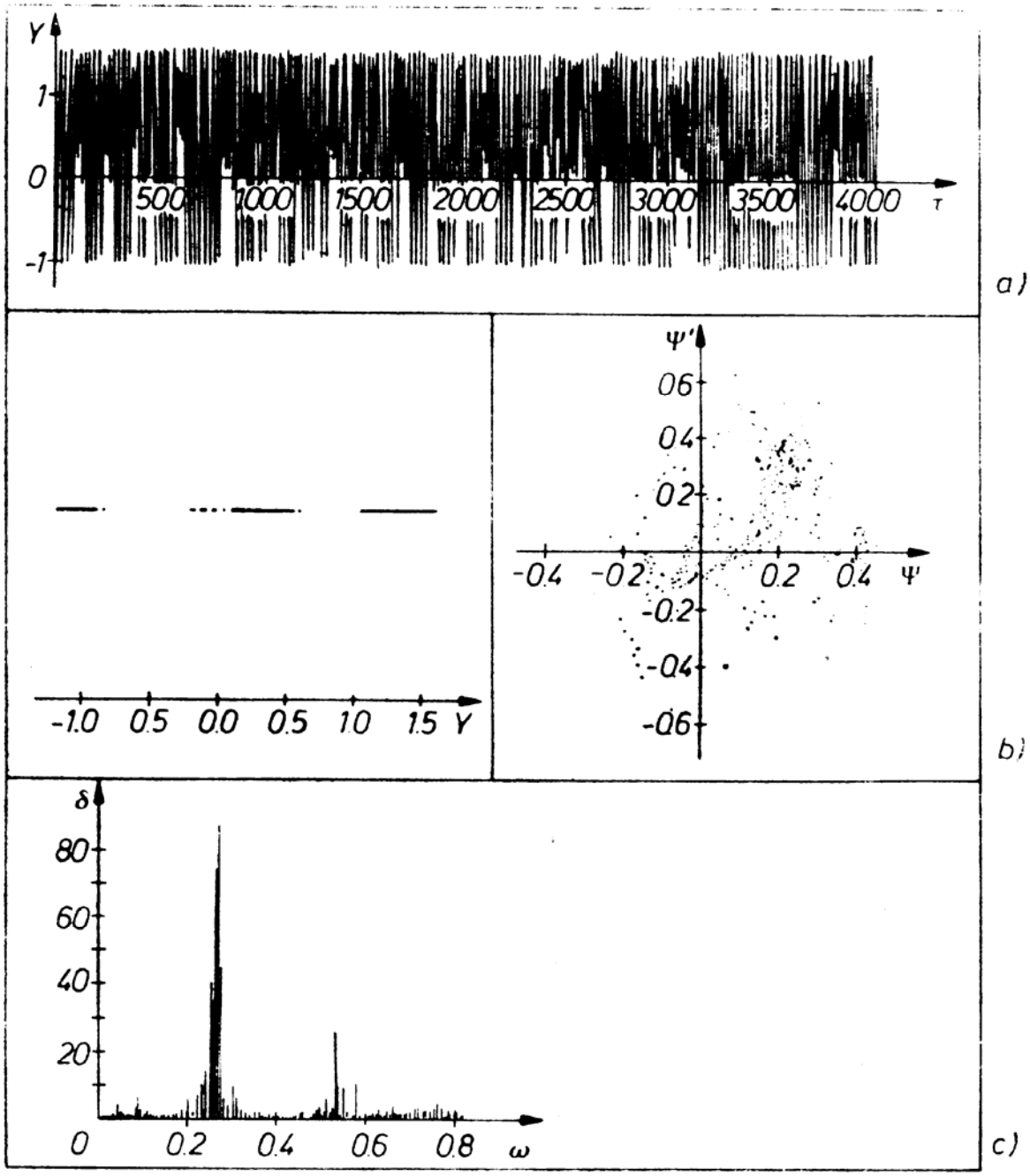
Y
1
0
-1
500
1000
1500
2000
2500
3000
3500
4000
τ
a)
-1.0
0.5
0.0
0.5
1.0
1.5
Y
Ψ'
06
04
02
-0.4
-0.2
0.2
0.4
Ψ
-0.2
-0.4
-06
b)
δ
80
60
40
20
0
0.2
0.4
0.6
0.8
ω
c)

[Eig. 5a b c]

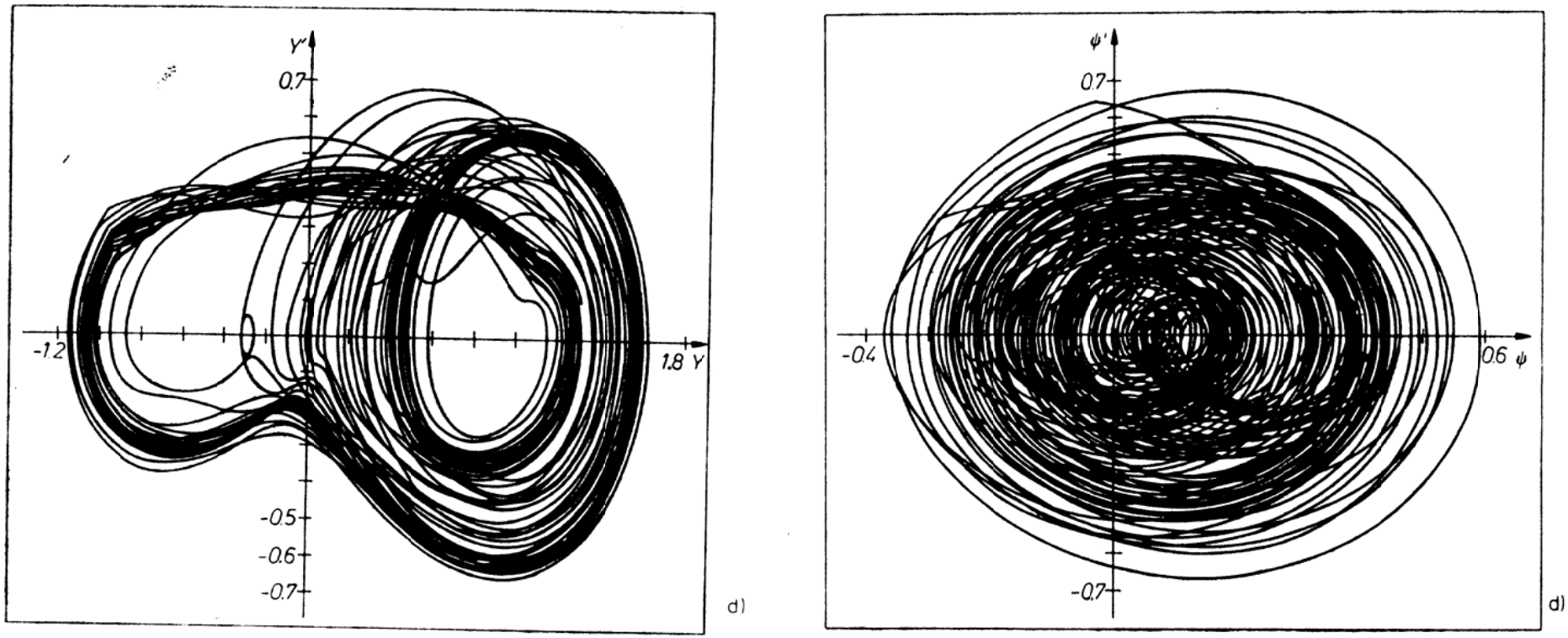

FIG. 5. Intermittency chaos for $\gamma = 0.836$ and $y_0 = 0.409$, $y_0' = -0.11$, $\psi_0 = 0.095$, $\psi_0' = 0.416$ a) time history; b) Poincarč' map projection ($y' = 0$); c) power spectrum of $y(\tau)$; phase portraits.

For the stick-state we have

$$y_1' = y_2,$$

$$y_2' = -\frac{1}{(\vartheta+1)}\left[\left(1-\left(\frac{\chi}{\lambda}\right)^2\right)\beta_1 y_2+\left(1-\frac{1}{\lambda}\right)y_1-\frac{1}{\varrho\vartheta}\left(1+\frac{\chi}{\varrho}\frac{1}{\lambda^2}\right)(\beta_2 y_4+\varkappa y_3)\right],$$

$$y_5' =: 1,$$

where

$$y_3 = y_{3H}+\vartheta\varrho\left\{v_B(\tau-\tau_H)-(y_1-y_{1H})-\frac{1}{\varrho}\arctan\left(\frac{y_1}{\chi}\right)+\frac{1}{\varrho}\arctan\left(\frac{y_{1H}}{\chi}\right)\right\},$$

$$y_4 = \vartheta\varrho\left\{v_B-\left(1+\frac{\chi}{\varrho}\frac{1}{\lambda^2}\right)y_2\right\},$$

$$y_5 = \tau.$$

Numerical calculations have been made for the following fixed parameters: $\chi = 0.6$, $\varrho = 2.5$, $v_B = 0.5$, $v^* = 1.0$, $\varkappa = 1.0$, $\beta_1 = \beta_2 = 0.05$, $\mu_1 = 0.05$, $\mu_2 = 0.2$, $\vartheta = 0.5$. γ has been chosen as the bifurcation parameter. Its influence on the dynamics of the system considered appears to be the most important as its change affects the change of mass and the mass moment of inertia of the disc and the change of the normal and friction forces. A periodic orbit has been found for $\gamma = 0.5$ (Fig. 4a) using the method based on solution of the boundary value problem, and then its changes accompanying the increase of γ have been followed. For $\gamma = 0.60946$ one of the characteristic multipliers reaches the value of -1 and the further increase of γ causes the loss of stability of the analyzed orbit and in the bifurcation point a new periodic orbit branches, with its period two times greater than that of the original one (Fig. 4b). The new orbit does not double its period with the increase of γ. For $\gamma = 0.6995$, when one of the characteristic multipliers reaches the value of $+1$, it disappears due to bifurcation and, instead, a chaotic orbit appears. That it is a chaotic one is well proved by irregular time histories, points of Poincaré map forming a strange structure, and continuous frequency spectrum, as well as attractor projections on planes $Y'(Y)$ and $\psi'(\psi)$ (Figs. 5 and 6).

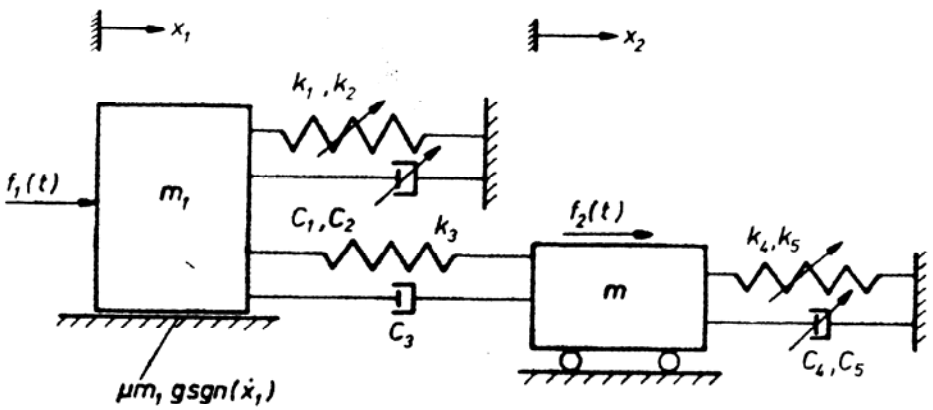

FIG. 6. Nonautonomous system with two degrees of freedom.

5. Vibrations in a Nonautonomous System with Friction

Let us consider a system of two mechanical oscillators coupled by a flexible and damping linear element [10]. Moreoven, each of them is harmonically excited and one is affected by dry friction. The equations governing the dynamics of these two coupled oscillators are

$$m_1\ddot{x}_1+(c_3-c_1(\dot{x}_1-c_2\dot{x}_2+c_2x_1^2\dot{x}_1+(k_1+k_3)x_1-k_2x_2+k_2x_1^3+ \\ +\mu m_1 g sgn(\dot{x}_1) = q_1\cos\omega_1 t,$$

$$m_2\ddot{x}_2+(c_3-c_4)\dot{x}_2-c_3\dot{x}_1+c_5x_2^2\dot{x}_2+(k_3+k_4)x_2-k_3x_1+k_5x_2^3 = q_2\cos\omega_2 t. \tag{5.1}$$

When $\dot{x}_1 = 0$ and $|F| < |F_s|$, where

$$F_s = \mu m_1 g, \\ F = (k_1+k_3)x_1-k_2x_2+k_2x_1^3-c_3\dot{x}_2-q_1\cos\omega_1 t, \tag{5.2}$$

the oscillator 1 (with the mass m_1) stops. In this stick-state the system is governed by the equations

$$\dot{x}_1 \equiv 0, \quad x_1 = \text{const}, \\ m_2\ddot{x}_2+(c_5-c_4)\dot{x}_2+c_5x_2^2\dot{x}_2(k_4+k_3)x_2-k_3x_1+k_5x_2^3 = q\cos\omega_2 t. \tag{5.3}$$

The oscillator 1 starts to slide if $|F|-|F_s| > 0$ and Eq. (5.1) again govern the behaviour of the system.

In order to reduce the parameter space and to extend the numerical results for the possibly other physical systems we transform Eq. (5.1) into the nondimensional form,

$$\ddot{\xi}_1+(\alpha_3-\alpha_1)\xi_1-\alpha_3(K/M)^{1/2}\dot{\xi}_2+\gamma_1\dot{\xi}_1^2\xi_1+(\varkappa_1+\varkappa_3)\xi_1-\varkappa_3(K/M)^{1/2}\xi_2+\zeta_1^3+ \\ +R\,\mathrm{sgn}(\dot{\xi}_1) = B_1\cos\tau, \\ \ddot{\xi}_2+M(\alpha_3-\alpha_4)\dot{\xi}_2-\alpha_3M^{3/2}K^{-1/2}\dot{\xi}_1+\gamma_2K\xi_2^2\dot{\xi}_2+M(\varkappa_3+\varkappa_4)\xi_2-M^{3/2}\varkappa_3K^{-1/2}\xi_1+ \\ +\xi_2^3 = M^{3/2}K^{-1/2}B_2\cos\nu\tau, \tag{5.4}$$

where

$$\tau = \omega_1 t, \quad \xi_1 = (\omega_1 m_1^{-1})k_2^{1/2}x_1, \quad \xi_2 = (\omega_1 m_2)^{-1}k_5^{1/2}x_2, \quad M = m_1m_2^{-1}, \\ K = k_2k_5^{-1}, \quad \nu = \omega_2\omega_1^{-1}, \quad B_1 = q_1\omega_1^{-3}m_1^{-3}k_2^{1/2}, \quad B_2 = q_2\omega_1^{-3}m_2^{-3}k_2^{1/2}, \\ \alpha_1 = c_1(m_1\omega_1)^{-1}, \quad \alpha_3 = c_3(m_1\omega_1)^{-1}, \quad \alpha_4 = c_4(m_1\omega_1)^{-1}, \quad \gamma_1 = \omega_1c_2k_2^{-1}, \\ \gamma_2 = \omega_1c_4k_2^{-1}, \quad \varkappa_1 = k_1m_1^{-1}\omega_1^{-1}, \quad \varkappa_3 = k_3m_1^{-1}\omega_1^{-2}, \quad \varkappa_4 = k_4m_1^{-1}\omega_1^{-2}, \\ R = \mu g\omega_1^{-3}k_2^{1/2}m_1^{-1}. \tag{5.5}$$

In the case of the stick we have

$$\xi_1 \equiv 0, \\ \ddot{\xi}_2+M(\alpha_3-\alpha_4)\dot{\xi}_2+\gamma_2K\xi_2^2\dot{\xi}_2+M(\varkappa_3+\mu_4)\xi_2-M^{3/2}\varkappa_3K^{-1/2}\xi_1+\xi_2^3 = \\ = M^{3/2}K^{-1/2}B_2\cos\tau, \tag{5.6}$$

and the condition for the transition to stick-state is

$$R > |(\varkappa_1+\varkappa_3)\xi_1-\varkappa_3(K/M)^{1/2}\xi_2+\xi_1^3-\alpha_3(K/M)^{1/2}\dot{\xi}_2-Bc_1\cos\tau|. \tag{5.7}$$

The considered system has a periodic solution for the following parameters: $\nu = 1.0$, $M = K = 1.0$, $\varkappa_1 = \varkappa_4 = -0.8163$, $\gamma_1 = \gamma_2 = 0.3$, $B_1 = 0.05$, $B_2 = 0.2$, $R = 0.05$, $\alpha_1 = \alpha_4 = 0.05$, $\alpha_3 = \varkappa_3 = 0.3$. The transient state shortly before the periodic orbit is reached is shown in Fig. 7. The increase of $\alpha_1 = \alpha_4$ causes the increase of the self-excited

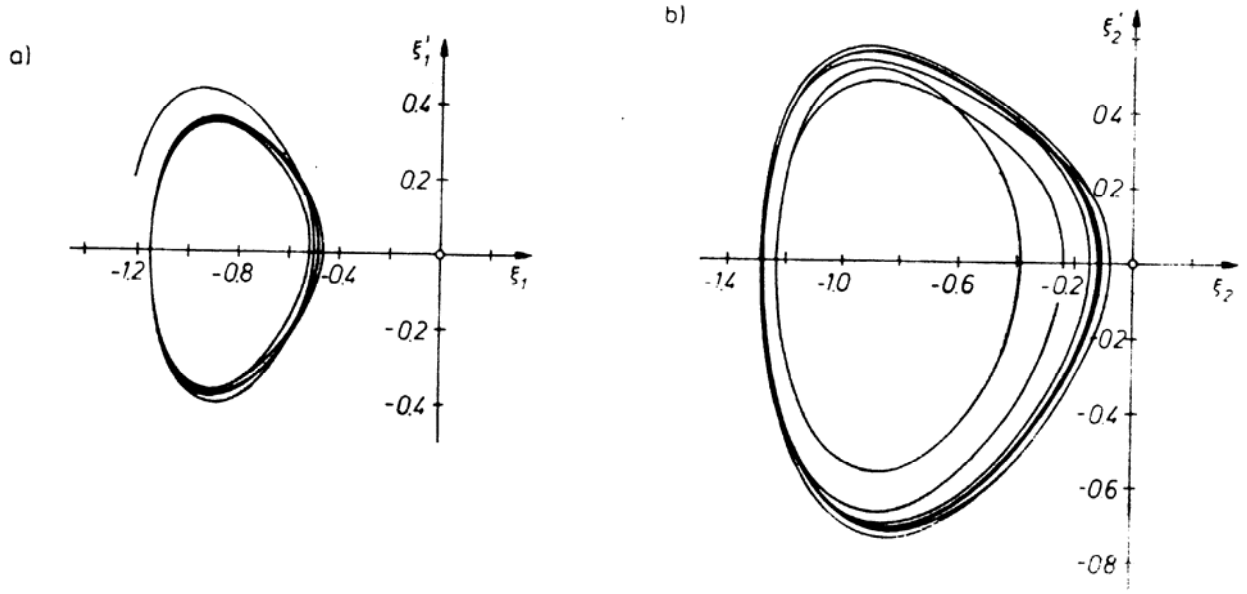

FIG. 7. Phase portraits of the trajectory approaching 2π-periodic orbit in the nonautonomous system.

vibrations quantity. The periodic orbit situated on the left-hand side of the origin of coordinates increases (the periodic orbit on the right-hand side of the origin of coordinates bahaves similarly). A further increases of $\alpha_1 = \alpha_4$ leads to the loss of stability of the considered orbits and the trajectory starts to wander in an unpredictable way between two potential wells. This situation is presented in Fig. 8.

6. Concluding Remarks

The paper presents three different routes to chaos as shown in the three presented physical systems. In the case of the equation system governing the vibrations of human vocal cords we have demonstrated the transition from a periodic to quasiperiodic orbit, and after bifurcation of the latter—to chaos.

In the second self-excited mechanical system with two degrees of freedom it has been shown that although the considered periodic orbit doubles its period with the change of bifurcation parameter, this does not lead to an infinite sequence of period-doubling bifurcations (which could be noticed when analysing three-dimensional systems). The newly-created orbit disappears by means of saddle-node bifurcation and chaos is created.

Finally, the third route to chaos presented on the example of vibrations of a nonautonomous mechanical system with two degrees of freedom is the same as observed when analysing a single harmonically-excited oscillator.

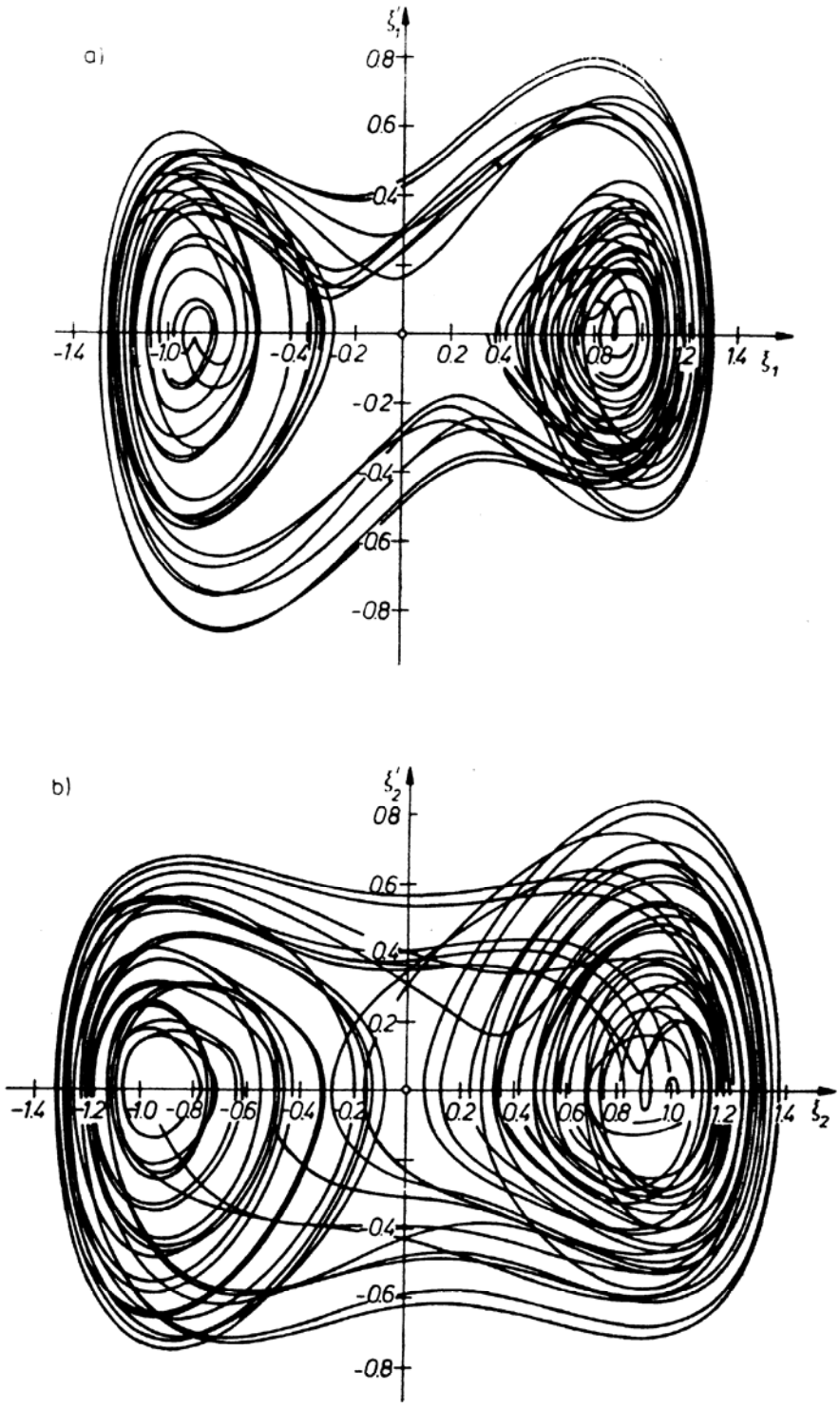

FIG. 8. Two projections of the strange chaotic attractor in nonautonomous system ($\alpha_1 = \alpha_4 = 0.2$).

Acknowledgement

This paper is based on the research which the author conducted in the course of his stay at the Technical University of Braunschweig under the terms of the Alexander von Humboldt Foundation Scholarship.

References

1. J. Guckenheimer, P. J. Holmes, *Nonlinear oscillations, dynamical systems and bifurcations of vector fields*, Springer–Verlag, New York 1983.
2. J. M. T. Thompson, H. B. Stewart, *Nonlinear dynamics and chaos*, John Wiley and Sons, New York 1986.
3. J. Awrejcewicz, *Chaos in simple mechanical systems with friction*, J. Sound Vibr., 109(1), 178 - 180, 1986.
4. J. Awrejcewicz, *A route to chaos in a nonlinear oscillator with delay*, Acta Mech., 77, 111 - 120, 1989.
5. J. Awrejcewicz, *Two kinds of evolution of strange attractors for the example of a particular nonlinear oscillator*, J. Appl. Math. Phys. ZAMP, 40, 375 - 386, 1989.
6. J. Awrejcewicz, *Bifurcation and chaos in simple dynamical systems*, World Scientific, Singapore 1989.
7. V. I. Arnold, *Geometrical methods in the theory of ordinary differential equations*, Springer–Verlag, New York 1983.
8. R. Cronjaeger, *Die Entstehung des primaren Stimmklangs im menschlichen Kehlkopf-ein Modell*, Doctoral Thesis, Braunschweig 1978.
9. J. Awrejcewicz, J. Delfs, *Dynamics of a self-excited stick-slip oscillator with two degrees of freedom, Part 2. Periodic and chaotic orbits*, Eur. J. Mech. (to appear)
10. W.-D. Reinhardt, *Einfluss einer zweiten Masse auf die chaotische Bewegung eines nichtlinearen Feder-Masse-Schwingers*, MSc Thesis prepared under the supervision of J. Awrejcewicz, Branschweig 1989

Streszczenie

DROGI DO CHAOSU W ZŁOŻONYCH UKŁADACH FIZYCZNYCH

W pracy dokonano analizy przejść od ruchu regularnego do chaotycznego na bazie trzech złożonych układów fizycznych. Orbity okresowe śledzone były na podstawie rozwiązania problemu brzegowego, natomiast atraktory quasi-okresowe i chaotyczne na podstawie rozwiązania zagadnienia warunków początkowych (przebiegi czasowe, rzuty atraktora na wybrane płaszczyzny, mapy Poincaré, widma częstości czy maksymalny wykładnik Lapunowa). Pokazano, że przejścia od ruchu regularnego do nieregularnego w układach złożonych mogą być podobne lub różne od przejść spotykanych w prostych oscylatorach wymuszonych sinusoidalnie.

Резюме

ПУТИ К ХАОСУ В СЛОЖНЫХ ФИЗИЧЕСКИХ СИСТЕМАХ

В работе проведен анализ переходов от регулярного движения к хаотическому на основе трех сложных физических систем. Периодические орбиты были слежены, опираясь на решение краевой задачи, а квазипериодические и хаотические аттракторы, опираясь на решение задачи начальных условий (временные процессы, проекции аттрактора на избранные плоскости, карты Пуанкаре, спектры частоты или максимальный показатель Ляпунова). Показано, что переходы от регулярного к нерегулярному движению в словжных системах могут быть аналогичными или разными от переходов встречаемых в простых вынужденных синусоидально осцилляторах.

INSTITUTE OF APPLIED MECHANICS
TECHNICAL UNIVERSITY OF ŁÓDŹ.

Received December 28, 1989.